



# Potential Application of B<sub>40</sub> Fullerene as an Innovative Anode Material for Ca-ion Batteries: *In Silico* Investigation

Elham Tahmasebi

Chemistry Department, Faculty of Science, Shahid Chamran University of Ahvaz, Ahvaz, Iran

Ehsan Shakerzadeh 

Chemistry Department, Faculty of Science, Shahid Chamran University of Ahvaz, Ahvaz, Iran

Received: 17 June 2020 / Accepted: 24 June 2020 / Published Online: 30 June 2020

Copyright © 2020 to Lab-in-Silico as a Member of SciEng Publishing Group (SciEng)


**ABSTRACT.** Density functional theory (DFT) calculations were performed using the PBE0-D3 functional and the 6-31+G(d) basis set to determine the potential application of recent experimentally observed B<sub>40</sub> fullerene for the anode electrode for Ca-ion batteries (CIBs) *in silico*. The interactions of both Ca and Ca<sup>2+</sup> with the B<sub>40</sub> fullerene were investigated for the purpose. Based on the calculated results, the bare B<sub>40</sub> fullerene have been seen as a promising anode material with remarkable average open-circuit voltage of 4.52 V and storage capacity of 744 mAhg<sup>-1</sup>. The obtained results of this study might open new windows for designing such promising boron-based anode materials for CIBs, which is an advantage of computer-based works for novel technologies. Such novel types of batteries are very much important to be developed for applications in high level technologies and industries.

**KEYWORDS.** B<sub>40</sub> fullerene; Open-circuit voltage; Ca-ion batteries; DFT calculations.

**INTRODUCTION.** Rechargeable batteries are electrical energy storages, which could generate clean energy and accordingly decrease fossil fuel consumption to reduce production of the hazardous greenhouse gases.<sup>1-7</sup> Lithium-ion batteries (LIBs) as the first type of secondary batteries, have been used commonly in various electronic devices of modern technologies.<sup>7-11</sup> However, LIBs are suffered from low voltage energy storage, high price and limited available lithium resources.<sup>12</sup> Accordingly, novel rechargeable batteries on the basis of earth-abundant metals (i.e., Mg, Na, Ca, Al, and K) have arisen extensive interests of researchers.<sup>13-21</sup> Specifically, calcium-ion batteries (CIBs) are considered to be promising next-generation energy storage systems because of the natural abundance of calcium and the multivalent calcium ions with low redox potential close to that of lithium, which

are all advantages for Ca atom for such application in batteries.<sup>22, 23</sup>

Boron compounds with specially enviable physicochemical properties and promising applications have received incessant attention of several research areas.<sup>24-27</sup> Research on boron clusters and their various applications are intriguing fields for both experimental and theoretical chemists.<sup>28, 29</sup> The new experimentally observed all-boron (B<sub>40</sub>) fullerene with D<sub>2d</sub> symmetry was found to be the most stable allotrope.<sup>30</sup> Numerous studies have been focused on the doped B<sub>40</sub> fullerenes with different transition metals or other atoms to further improve their electronic, optical and structural characteristic features.<sup>31-33</sup> For instance, the structural stability properties for MB<sub>40</sub> (M = Li, Na, K, Ba, and Tl) were investigated through density functional theory (DFT) calculations with particular attention on the

 Corresponding author; E-mail address: e.shakerzadeh@scu.ac.ir (E. Shakerzadeh).

relative stability between the endohedral and exohedral configurations.<sup>33</sup> Accordingly, the Na and Ba atoms are stably encapsulated inside the B<sub>40</sub> fullerene, whereas the Li, K, and Tl atoms prefer the exohedral configuration. Also, Fai et al.<sup>34</sup> reported an exohedral complexation of Mg and Be metals with B<sub>40</sub> fullerene. Moradi et al.<sup>35</sup> in 2017 investigated the interaction of Li and Li<sup>+</sup> with a B<sub>40</sub> fullerene using DFT method for its possible application as an anode of LIBs and the cell voltage was reported to be 0.53 V. Indeed, the advances of nanotechnology approach yielded several other related phenomena to investigate materials for novel application.<sup>36-40</sup> Additionally, *in silico* approach provided reliable methods to perform computer-based research works in parallel with experiments.<sup>41-45</sup>

In such view of designing appropriate anode for CIBs, it is of interest to investigate the potential possibility of B<sub>40</sub> fullerene (Fig. 1) as an anode of CIBs. The main objective of this work is an assessment of the Ca and Ca-ion interaction with B<sub>40</sub> fullerene and evaluation of its performance for an anode of CIBs. Furthermore, the effect of halides anion (F<sup>-</sup>, Cl<sup>-</sup>, and Br<sup>-</sup>) encapsulation inside B<sub>40</sub> fullerene on its efficiency for an anode electrode of CIBs is studied. This study could provide a comprehensive understanding of the promising boron-based anode for CIBs and a concrete suggestion to take forward for its eventual experimental applications.

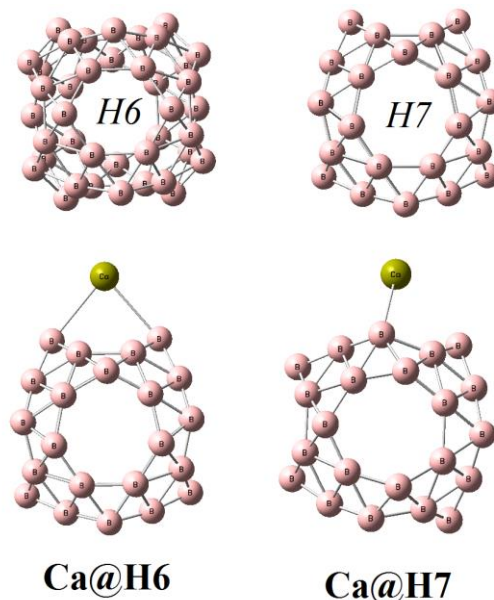


Fig. 1: Relaxed geometries of B<sub>40</sub> and Ca@B<sub>40</sub> structures.

**METHODOLOGY.** Geometrical optimizations were performed using the PBE0-D3/6-31+G(d) level of DFT calculations. The vibrational frequencies were also calculated at the same level to confirm the identity of the ground state avoiding the existence of imaginary frequency. The employed functional showed reliable results for such system based on the achievements of earlier works.<sup>46</sup> All calculations were carried out using the Gaussian 09 suite of program.<sup>47</sup> All considered structures were stabilized at the singlet state with multiplicity ( $M$ ) of one ( $M=2S+1$ ,  $S$ = total spin).

**Table 1:** Calculated HOMO ( $E_{\text{HOMO}}$ ), LUMO ( $E_{\text{LUMO}}$ ), HOMO-LUMO gap (HLG), interaction energy ( $E_{\text{int}}$ ), and average open-circuit cell voltage ( $V_{\text{oc}}$ ).

Models	$E_{\text{HOMO}}$ (eV)	$E_{\text{LUMO}}$ (eV)	HLG (eV)	$E_{\text{int}}$ (kcal/mol)	$V_{\text{oc}}$ (Volt)
B <sub>40</sub>	-6.38	-3.26	3.12	N/A	N/A
H6-Ca@B <sub>40</sub>	-4.61	-2.97	1.64	-33.44	1.83
H6-Ca <sup>2+</sup> @B <sub>40</sub>	-11.94	-9.60	2.34	-118.02	N/A
H7-Ca@B <sub>40</sub>	-4.46	-3.05	1.41	-34.88	2.01
H7-Ca <sup>2+</sup> @B <sub>40</sub>	-12.12	-9.39	2.73	-127.54	N/A

**RESULTS & DISCUSSION.** Fig. 1 displays the relaxed geometry of B<sub>40</sub> fullerene with the D<sub>2d</sub> point group, obtained at the PBE0-D3/6-31+G(d) level of DFT calculations. This fullerene structure was consisted of two staggered hexagonal holes (H6) at the top and bottom and four inverted heptagonal holes (H7) evenly distributed around the waist. The highest occupied and the lowest unoccupied molecular orbital (HOMO and LUMO) energies and their energy difference value (HOMO-LUMO gap) of the investigated original B<sub>40</sub>

fullerene structure were calculated to be -6.38, -3.26 and 3.12 eV, respectively (Table 1). Next, the complexation process of calcium (Ca) metal in the neutral and di-cationic states with the B<sub>40</sub> were considered. The energetically favorable complexes were found by checking all probable positions (i.e., atop of H6 and H7, above individual boron atoms, and different distinguishable B-B bonds). Full geometrical optimizations revealed that both neutral and di-cationic metals could relax above the H7 and H6 holes

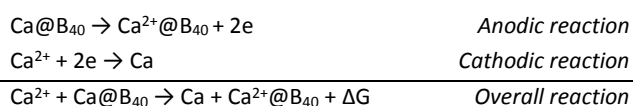
(Fig. 1). The thermodynamic stability of the obtained complexes were assessed by calculation of interaction energies ( $E_{\text{int}}$ ) as shown in the Eq. (1):

$$E_{\text{int}} = E_{\text{Ca}^{0/2+} @ \text{B}_{40}} - (E_{\text{B}_{40}} + E_{\text{Ca}^{0/2+}}) \quad (1)$$

where  $E_{\text{Ca}^{0/2+} @ \text{B}_{40}}$  represents the total energy of the metal@B<sub>40</sub> complex in neutral or di-cationic states.  $E_{\text{B}_{40}}$  and  $E_{\text{Ca}^{0/2+}}$  denote the corresponding energies of the bare B<sub>40</sub> and single neutral or di-cationic metal atom, respectively. It is noted that the complex with high  $E_{\text{int}}$  has significant stability. All the calculated parameters for the models (Fig. 1) were summarized in Table 1.

Examining the obtained results indicated that Ca<sup>2+</sup> cation had a substantially stronger interaction with the B<sub>40</sub> in comparison with the neutral Ca metal. Furthermore, complex formation of both neutral and di-cation metal with H7 were influential than their interaction with H6. The obtained interaction energies of H7-Ca<sup>2+</sup>@B<sub>40</sub> and H6-Ca<sup>2+</sup>@B<sub>40</sub> were calculated to be -127.54 and -118.02 kcal/mol indicating their remarkable high stability. On the other hand, the corresponding interaction energies were -34.88 and -33.44 kcal/mol for H7-Ca@B<sub>40</sub> and H6-Ca@B<sub>40</sub> complexes, respectively. The average distance of Ca and Ca<sup>2+</sup> with B atoms of H6 or H7 were measured to be 2.87 and 2.83 Å, respectively. The shorter interaction distance of Ca<sup>2+</sup> with H7 or H6 than Ca metal was in correlation with higher interaction energies of these complexes. Also, B-B bonds of H6 or H7 slightly (~0.02 Å) elongated by interaction with Ca or Ca<sup>2+</sup>. Additionally, B1....B9 and B2....B10 distances in H7 and H6 were considered as diameter of H7 ( $d_{\text{H7}}$ ) and H6 ( $d_{\text{H6}}$ ). Both diameters of H7 and H6 ( $d_{\text{H7}}$  and  $d_{\text{H6}}$ ) were increased from 3.49 and 3.38 Å to 3.67 (3.63) and 3.46 (3.40) Å due to Ca (Ca<sup>2+</sup>) interactions. It turned out that H7 hole was expanded more than H6 one during interaction with Ca or Ca<sup>2+</sup>.

By motivating for doing further investigation of the B<sub>40</sub> capability for introducing as an anode for CIBs, details of such typical metal-ion battery could be assumed as below, in which the electrochemical reactions at anode and cathode of a metal-ion could be shown:



The average open circuit intercalation potential ( $V_{\text{oc}}$ ) is one of the key parameters to determine the performance of batteries. Theoretically,  $V_{\text{oc}}$  could be evaluated on the basis on Nernst equation given by:

$$V_{\text{oc}} = \frac{-\Delta G}{zF} \quad (2)$$

The Faraday constant ( $F$ ) is 96500 C.mol<sup>-1</sup> and  $z=2$  denotes the charge of the working ion in electrolyte (i.e. Ca<sup>2+</sup>).  $\Delta G$  term is the difference of the Gibbs free energy for overall reaction, which could be estimated from the internal energy ( $E$ ) by neglecting the changes in volume and entropy:

$$\Delta G = \Delta E + P\Delta V - T\Delta S \approx \Delta E \quad (3)$$

Therefore,  $V_{\text{oc}}$  of a CIB could be written by Eq. (4):

$$V_{\text{oc}} = \frac{-(E_{\text{Ca}^{2+} @ \text{B}_{40}} + E_{\text{Ca}} - E_{\text{Ca} @ \text{B}_{40}} - E_{\text{Ca}^{2+}})}{2F} \quad (4)$$

The average open circuit voltage was calculated by obtained energies ( $E$ ) of the considered species. Accordingly, this result indicated that high  $V_{\text{oc}}$  could be evaluated from the stronger interaction of working ion metal with B<sub>40</sub> compared to the neutral metal. Since the Ca<sup>2+</sup> interaction with B<sub>40</sub> was much stronger than Ca, it was found that B<sub>40</sub> fullerene could be a potential promising anode material for CIBs. Calculated  $V_{\text{oc}}$  for Ca interaction with H7 and H6 of B<sub>40</sub> were 2.01 and 1.83 V, respectively.

The storage capacity ( $C$ ) is another key factor for studying the performance of CIBs, which could be computed from Faraday equation; Eq. (5):

$$C(\text{mAhg}^{-1}) = \frac{(n_{\text{max}} \times k \times F \times 10^3)}{M_{\text{anode}}} \quad (5)$$

where  $n_{\text{max}}$ ,  $k$  and  $F$  terms stand for the maximum number of adsorbed Ca metals, the valence electron number (2 for Ca), and the Faraday constant (26.81 Ahmol<sup>-1</sup>).  $M_{\text{anode}}$  is the atomic mass of B<sub>40</sub> fullerene. In order to find the storage capacity, we examined the Ca interaction with all six possible holes of B<sub>40</sub>, because the Ca interacted markedly with both of H6 and H7. Resulting 6Ca@B<sub>40</sub> was found to be a true local minimum with no imaginary frequency. Each Ca atom relaxed above H6 and H7 holes. This structure was also optimized in di-cationic state for the calculation of cell voltage. Accordingly,  $V_{\text{oc}}$  was found to be 4.52 V, which was more significant than those values for singular Ca decoration of B<sub>40</sub> fullerene. Furthermore, the

theoretical storage capacity of 744 mAhg<sup>-1</sup> was obtained large enough to make B<sub>40</sub> a good candidate as the anode material for CIBs. As discussed above, B<sub>40</sub> fullerene could adsorb six Ca atoms, providing both remarkable average open-circuit voltage and storage capacity. Consequently, both high V<sub>oc</sub> and storage capacity parameters demonstrated that the B<sub>40</sub> fullerene could be regarded as potential promising candidates for the anode of CIBs.

**CONCLUSION.** Within this theoretical study *in silico*, we studied the interaction of Ca and Ca<sup>2+</sup> with the B<sub>40</sub> fullerene. The obtained results indicated that

the Ca<sup>2+</sup> interaction with heptagonal and hexagonal holes of B<sub>40</sub> fullerene was much stronger than Ca metal. The open circuit voltage obtained to be as a considerable value of ~2.0 V. To obtain the storage capacity of B<sub>40</sub> fullerene, all six holes of B<sub>40</sub> had decorated with Ca metals and the V<sub>oc</sub> and storage capacity were found to be 4.52 V and 744 mAhg<sup>-1</sup>, respectively. Current results might be helpful in designing new boron-based materials with even better energy storage density. Accordingly, the B<sub>40</sub> fullerene might be a plausible candidate for application as an anode material of Ca-ion batteries based on the achievements of this computer-based work.

## REFERENCES

- Dunn B, Kamath H, Tarascon JM. Electrical energy storage for the grid: A battery of choices. *Science*. 2011;334:928-935.
- Soloveichik GL. Battery technologies for large-scale stationary energy storage. *Ann Rev Chem Biomol Engin*. 2011;2:503-527.
- Cheng F, Liang J, Tao Z, Chen J. Functional materials for rechargeable batteries. *Adv Mater*. 2011;23:1695-1715.
- Liu C, Li F, Lai-Peng M, Cheng HM. Advanced materials for energy storage. *Adv Mater*. 2010;22(8):28-62.
- Duffner F, Wentker M, Greenwood M, Leker J. Battery cost modeling: A review and directions for future research. *Renew Sustain Energy Rev*. 2020;127:109872.
- Raccichini R, Varzi A, Passerini S, Scrosati B. The role of graphene for electrochemical energy storage. *Nat Mater*. 2015;14:271-279.
- Chan CK, Peng H, Liu G, McIlwrath K, Zhang XF, Huggins RA, et al. High-performance lithium battery anodes using silicon nanowires. *Nat Nanotechnol*. 2008;3:31-35.
- Ma C, Shao X, Cao D. Nitrogen-doped graphene nanosheets as anode materials for lithium ion batteries: A first-principles study. *J Mater Chem*. 2012;22:8911-5.
- Goodenough JB, Park KS. The Li-ion rechargeable battery: A perspective. *J Am Chem Soc*. 2013;135:1167-1176.
- Opitz A, Badami P, Shen L, Vignarooban K, Kannan AM. Can Li-Ion batteries be the panacea for automotive applications? *Renew Sustain Energy Rev*. 2017;68:685-92.
- O'Heir J. Building better batteries. *Mech Eng*. 2017;139:10-11.
- Wang R, Cui W, Chu F, Wu F. Lithium metal anodes: Present and future. *J Energy Chem*. 2020;48:145-159.
- Mukherjee S, Singh G. Two-dimensional anode materials for non-lithium metal-ion batteries. *ACS Appl Energy Mater*. 2019;2:932-955.
- Wang Y, Chen R, Chen T, Lv H, Zhu G, Ma L, et al. Emerging non-lithium ion batteries. *Energy Storage Mater*. 2016;4:103-129.
- Chen X, Wang S, Wang H. High performance hybrid Mg-Li ion batteries with conversion cathodes for low cost energy storage. *Electrochim Acta*. 2018;265:175-183.
- Nejati K, Hosseini A, Bekhradnia A, Vessally E, Edjlali L. Na-ion batteries based on the inorganic BN nanocluster anodes: DFT studies. *J Mol Graph Model*. 2017;74:1-7.
- Benzidi H, Lakhali M, Garara M, Abdellaoui M, Benyoussef A, El Kenz A, et al. Arsenene monolayer as an outstanding anode material for (Li/Na/Mg)-ion batteries: Density functional theory. *Phys Chem Chem Phys*. 2019;21:19951-19962.
- Kosar N, Asgar M, Ayub K, Mahmood T. Halides encapsulation in aluminum/boron phosphide nanoclusters: An effective strategy for high cell voltage in Na-ion battery. *Mater Sci Semicond Process*. 2019;97:71-79.
- Tao ZL, Xu LN, Gou XL, Chen J, Yuan HT. TiS<sub>2</sub> nanotubes as the cathode materials of Mg-ion batteries. *Chem Commun*. 2004;10:2080-2081.
- Aslanzadeh SA. A computational study on the potential application of zigzag carbon nanotubes in Mg-ion batteries. *Struct Chem*. 2020; in press.
- Liu Y, Sun Z, Tan K, Denis DiK, Sun J, Liang L, et al. Recent progress in flexible non-lithium based rechargeable batteries. *J Mater Chem A*. 2019;7:4353-4382.
- Gummow RJ, Vamvounis G, Kannan MB, He Y. Calcium-ion batteries: Current state-of-the-art and future perspectives. *Adv Mater*. 2018;30:1-14.
- Park J, Xu Z, Yoon G, Park SK, Wang J, Hyun H. Stable and high-power calcium-ion batteries enabled by calcium intercalation into graphite. *Adv Mater*. 2020;32:1904411.
- Romanescu C, Galeev TR, Sergeeva AP, Li W-L, Wang L-S, Boldyrev AI. Experimental and computational evidence of octa- and nona-coordinated planar iron-doped boron clusters: Fe@B<sub>8</sub><sup>-</sup> and Fe@B<sub>9</sub><sup>-</sup>. *J Organomet Chem*. 2012;721:148-154.
- Jian T, Chen X, Li SD, Boldyrev AI, Li J, Wang LS. Probing the structures and bonding of size-selected boron and doped-boron clusters. *Chem Soc Rev*. 2019;48:3550-3591.

26. Popov IA, Jian T, Lopez G V., Boldyrev AI, Wang LS. Cobalt-centred boron molecular drums with the highest coordination number in the CoB<sub>16</sub><sup>-</sup> cluster. *Nat Commun.* 2015;6:1-7.
27. Zubarev DY, Boldyrev AI. Comprehensive analysis of boron clusters. *J Comput Chem.* 2007;28:251-268.
28. Pham HT, Duong L V., Nguyen MT. Electronic structure and chemical bonding in the double ring tubular boron clusters. *J Phys Chem C.* 2014;118:24181-24187.
29. Pham HT, Pham-Ho MP, Nguyen MT. Impressive capacity of the B<sub>7</sub><sup>-</sup> and V<sub>2</sub>B<sub>7</sub> clusters for CO<sub>2</sub> capture. *Chem Phys Lett.* 2019;728:186-194.
30. Zhai HJ, Zhao YF, Li WL, Chen Q, Bai H, Hu HS, et al. Observation of an all-boron fullerene. *Nat Chem.* 2014;6:727-731.
31. Yang Y, Zhang Z, Penev ES, Yakobson BI. B<sub>40</sub> cluster stability, reactivity, and its planar structural precursor. *Nanoscale.* 2017;9:1805-1810.
32. Maniei Z, Shakerzadeh E, Mahdavi Z. Theoretical approach into potential possibility of efficient NO<sub>2</sub> detection via B<sub>40</sub> and Li@B<sub>40</sub> fullerenes. *Chem Phys Lett.* 2018;691:360-365.
33. Fa W, Chen S, Pande S, Zeng XC. Stability of Metal-Encapsulating Boron Fullerene B<sub>40</sub>. *J Phys Chem A.* 2015;119:11208-11214.
34. Bai H, Chen Q, Zhai HJ, Li SD. Endohedral and exohedral metalloborospherenes: M@B<sub>40</sub> (M= Ca, Sr) and M@B<sub>40</sub> (M= Be, Mg). *Angew Chem.* 2015;54:941-945.
35. Moradi M, Bagheri Z, Bodaghi A. Li interactions with the B<sub>40</sub> fullerene and its application in Li-ion batteries: DFT studies. *Physica E.* 2017;89:148-54.
36. Mirzaei M. Nanotechnology for science and engineering. *Adv J Sci Eng.* 2020;1:67-68.
37. Faramarzi R, Falahati M, Mirzaei M. Interactions of fluorouracil by CNT and BNNT: DFT analyses. *Adv J Sci Eng.* 2020;1:62-66.
38. Ulfat I, Ahmed SA, Iqbal SMZ, Kamaluddin S, Mehmood Z, Kanwal S. Synthesis and characterization of gold nanoparticles. *Adv J Sci Eng.* 2020;1:48-51.
39. Ozkendir OM. Electronic structure study of Sn-substituted InP semiconductor. *Adv J Sci Eng.* 2020;1:7-11
40. Soleimanimehr H, Mirzaei M, Ghani M, Sattari F, Forouzan Najafabadi A. Micro-grooving of aluminum, titanium and magnesium alloys by acidithiobacillus ferrooxidans bacteria. *Adv J Sci Eng.* 2020;1:16-19.
41. Mirzaei M. The NMR parameters of the SiC-doped BN nanotubes: a DFT study. *Physica E.* 2010;42:1954-1957.
42. Mirzaei M. Lab-in-Silico: An international journal. *Lab-in-Silico.* 2020;1:1-2.
43. Harismah K, Mirzaei M. *In silico* interactions of steviol with monoamine oxidase enzymes. *Lab-in-Silico.* 2020;1:3-6.
44. Gunaydin S, Alcan V, Mirzaei M, Ozkendir OM. Electronic structure study of Fe substituted RuO<sub>2</sub> semiconductor. *Lab-in-Silico.* 2020;1:7-10.
45. Harismah K, Mirzaei M. Steviol and iso-steviol vs. cyclooxygenase enzymes: *In silico* approach. *Lab-in-Silico.* 2020;1:11-15.
46. Tian Y, Wei D, Jin Y, Barroso J, Lu C, Merino G. Exhaustive exploration of MgB<sub>n</sub> (n= 10-20) clusters and their anions. *Phys Chem Chem Phys.* 2019;21:6935-6941.
47. Frisch MJ, Trucks GW, Schlegel HB, Scuseria GE, Robb MA, Cheeseman JR, et al. Gaussian 09 A.01. Gaussian Inc., Wallingford; 2013.

**How to Cite:** Tahmasebi E, Shakerzadeh E. Potential Application of B<sub>40</sub> Fullerene as an Innovative Anode Material for Ca-ion Batteries: *In Silico* Investigation. *Lab-in-Silico.* 2020;1(1):16-20.

**DOI:** <https://doi.org/10.22034/labinsilico20011016>

**URL:** <https://sciengpub.com/lab-in-silico/article/view/labinsilico20011016>



This work is licensed under a [Creative Commons Attribution 4.0 International License \(CC-BY 4.0\)](https://creativecommons.org/licenses/by/4.0/).